East European Journal of Physics. 2. 159–172 (2025)
DOI: 10.26565/2312-4334-2025-2-16 ISSN 2312-4334

EVOLUTION OF KANTOWSKI-SACHS UNIVERSE WITH RENYI HOLOGRAPHIC DARK ENERGY

T. Chinnappalanaidu[a], **S. Srivani Madhu**[a], **M. Vijaya Santhi**[b], **N. Sri Lakshmi Sudha Rani**[b,c], **A. Krishna Rao**[d]

[a] *Department of Mathematics, Vignan's Institute of Information Technology (Autonomous), Visakhapatnam 530049, India*
[b] *Department of Applied Mathematics, Andhra University, Visakhapatnam 530003, India*
[c] *Department of Humanities and Sciences, Teegala Krishna Reddy Engineering College, Hyderabad-500097, India*
[d] *Department of Mathematics, Government Degree College, Chodavaram, Andhrapradesh, 531036, India*
* *Corresponding Author e-mail: chinnappalanaidu.tadi@gmail.com*

Received January 1, 2025; revised April 25, 2025; in final form May 14, 2025; accepted May 18, 2025

By considering generalized scalar tensor theory, as the gravitational theory, we have investigated the dynamical evolution of the homogeneous and anisotropic Kantowski-Sachs space in the presence of Renyi holographic dark energy. To obtain the solution for this model, we have derived the field equations and we have also analyzed the various physical and geometrical parameters of the model, such as deceleration, jerk, EoS, EoS plane, statefinder pair, density, squared speed of sound and the Om-diagnostic. It is shown from these parameters that the model is very much stable, projecting a quintessence nature and also, obtained model depicts the ΛCDM model. Our observations and conclusions from the constructed model are in good agreement with the recent studies.

Keywords: *Kantowski-Sachs metric; Anisotropic models; General scalar-tensor theory; Renyi holographic dark energy; Dark energy*

PACS: 98.80.-k; 95.36.+x

1. INTRODUCTION

The Universe we see today is around 46 billion light years in radius [1]. The formation of planets, stars and galaxies that keep changing over time, constitute the evolution of the cosmos. The American astronomer Edwin Powell Hubble has observed and deciphered that, from each direction, the distant stars and galaxies are moving away from Earth; and further, this rapid recession increases as the distance increases, implying that the Universe is expanding. Moreover, many repeated measurements have established these findings of Hubble ever since his discovery. Hubble's hypothesis of Universe expansion suggests that, all the presently observed matter and energy of the cosmos were more condensed as an infinitely small hot mass in the past, and later, a huge explosion called the "BIG BANG" has scattered the matter and energy in every direction. The Cosmic Microwave Background (CMB) explorer has confirmed that the background radiation field has the exact spectrum that is predicted by the Big Bang theory which prevails all the cosmological models and elucidates the Universe's initial development that begun 13.798 ± 0.037 billion years ago [2]. And, this hypothesis deduces that, in the deep space, the temperatures today, should be much more than the absolute zero. However, the modern astronomy is the consequence of Galileo's bequest of scientific knowledge of the space, and they understand that the present Universe has been made up of matter and vacuum. This view is widely held and appears to be common. Further experiments and observations made by the astronomers, the astrophysicists and, finally by particle physicists suggests that the Universe is much more beautiful and complicated than it was first believed. Additionally, general relativity tells that the past and as well the future of the Universe is depends on the aggregate of energy and matter contained therein. Hence, the study of exploded massive old stars has ascertained the existence of "dark matter (DM)" and the mysterious component called the "dark energy (DE)" which is neither related to matter nor energy and is clearly distinct from DM. These suggests that the space is being governed by the same physical laws all over its extent and history.

The observations from supernovae reveal that the there is an expanding Universe at an accelerating rate [3, 4]. Also, the Coma galaxy cluster mass [5, 6] along with the study of the galaxy rotation curve (1970) [7] that have been provided by the "Viral theorem" (1930's) has uncovered the most important aspects of cosmology: the dark sector (DM & DE),which is particularly accountable for rapid cosmic expansion and helps us to understand the nature of the cosmos. In terms of theological understanding, one of the most challenging issues is the concept of dark sectors [8]. For a standard cosmological scenario, the DM is called as cold dark matter (CDM), and DE as the cosmological constant (Λ). As a result of the combination of radiation and baryons, the ΛCDM model captures the dark component of the Universe. However, this is much of hypothetical nature, despite of ΛCDM having an impressive observational achievements [9, 10]. Taking some inspiration from the holographic principle [11–17], the idea of holographic dark energy (HDE) has been proposed by Li [18] to elucidate the phenomenon of rapid expansion of the Universe, in the year 2004. Consequently, the most complete generalization including the mostly known HDE models were suggested by Nojiri and Odintsov [19] and later

Cite as: T. Chinnappalanaidu, S. S. Madhu, M.V. Santhi, N.S.L.S. Rani, A.K. Rao, East Eur. J. Phys. 2, 159 (2025), https://doi.org/10.26565/2312-4334-2025-2-16

on, covariant theories different from Li's HDE have been discussed by Nojiri-Odintsov HDE [20]. Recently, a number of entropies have been formalized and are used to explore the various cosmological models. Among all those which are developed, namely Sharma Mittal HDE [21], Tsallis holographic dark energy (THDE) [22], Renyi holographic dark energy (RHDE) models [23] have proved to be more stable, based on non-interactions among the cosmic regions [24]. Current observations have suggested that Bekenstein entropy $\left(S = \frac{A}{4}\right)$ is nothing but Tsallis entropy [25–31] that ultimately lead to the following expression, for the ease of Renyi entropy [32] as,

$$S = \frac{1}{8}\log\left(\frac{\delta}{4}A + 1\right). \tag{1}$$

On applying equation (1), with the assumption $\rho_{de}dV \propto TdS$ [23], we acquire RHDE as

$$\rho_{de} = \frac{3c^2H^2}{8\pi\left(\frac{\pi\delta}{H^2} + 1\right)}, \tag{2}$$

where c^2 is a numerical constant. To obtain this we use relations that are reasonable in FLRW flat Universe [33], $T = \frac{H}{2\pi}$ and $A = \frac{4\pi}{H} = 4\pi\left(\frac{3V}{4\pi}\right)^{\frac{2}{3}}$. It is clear that without δ, we obtain $\rho_{de} = \frac{3c^2H^2}{8\pi}$, that agrees with the original HDE.

The RHDE models have been studied with various IR cut-offs [34, 35]. Furthermore, Sharma et al. [36, 37] have investigated how the RHDE model can be distinguished from the ΛCDM model using different diagnostic tools. More recently, Dubey and Sharma [38] have compared the holographic and THDE models with the RHDE model using the $(r\text{–}s)$ diagnostic. These studies highlight the importance of examining the interaction between dark energy (DE) and dark matter (DM). Additionally, constraints on the strength and nature of this interaction under different model setups have been explored in the literature [39–41]. Once again, the RHDE model in FLRW Universe has been investigated by Sharma and Dubey [42] by considering the interaction between the DM and DE. Also, RHDE model in a scalar tensor theory studied by Santhi and Naidu [43]. Very recently, Santhi et al., [44] have examined the RHDE model with two IR cutoffs in Saez-Ballester scalar tensor theory with marder type Universe.

It is assumed by many physicists that, at the emergence of the galaxies, the gravitational interactions responsible for the dynamics of the cosmos were quantized and its geometry should have been like a foam, resonating among the various configurations [45], which is of course, much different from what it is today. This raises the question on the validity of the "cosmological principle" which says that the Universe is homogeneous and isotropic, at sufficiently large scales [46]. Supposing that at the initial stages, the cosmological principle is not validated by the Universe i.e., the cosmos is inhomogeneous and anisotropic; and later it subsequently transformed to homogeneous and isotropic state as we understand it today. Since CMB radiation is almost uniformly distributed in all the directions with little variability, this transformation must have occurred before the matter and radiation got separated [47]. In a very transient period of time, cosmological inflation has caused the isotropization and homogenization of the primordial Universe, and later on with the initial singularity, the accelerated cosmic expansion has taken place and the size of the Universe has increased by many folds [48]. Physicists have worked on the proposition of inhomogeneous and anisotropic cosmos, turning into a homogeneous and isotropic one [49]. Most of these works are related to the initial time, where the Universe is homogeneous and anisotropic. However, one is left with many other possibilities to contribute for the choice of such a particular space-time. One such space time is the Kantowski-Sachs (KS) [50]. Therefore, the space-time S^2R spatial topology (or S^2S^1, when the real line is compactified because of identifications), has only two scale factors to describe the spherical symmetry. For this space-time we have constants and positives curvatures of the spatial slices. The KS space-time may also elucidate the Schwarzchild black hole in detail [50]. Many studies have been performed on this Universe by theorists, of which few have been mentioned here. The possibility of having a nonsingular KS-type static state has been evaluated by Ghorani and Heydarzade by considering four and five dimensional models [51]. The KS space time in the presence of strange quark matter cosmological models attached to string cloud in $f(R)$ theory of gravity has been examined by Santhi and Naidu [52]. A dynamical evolution of a homogeneous and anisotropic KS cosmological model has been studied by Oliveira-Neto in the presence of general relativity [53]. Observational constraints on RHDE in KS Universe has been studied by Prasanthi and Aditya [54]. The geometric properties of the generalized KS space-time, has been examined by Shaikh and Chakraborty [55], in a warped product of 2-dimensional base and fibre. Harmonic metrics with respect to generalized KS type space-times have been dealt with Altunbas [56]. The KS metric has been parameterized in a traditional way as:

$$ds^2 = dt^2 - A^2dr^2 - B^2(d\theta^2 + \sin^2\theta d\varphi^2), \tag{3}$$

where the arbitrary functions of time are taken as $A(t)$ and $B(t)$; and $r \in [0, +\infty)$ is the radial coordinate and θ, ϕ are the spherical angular coordinates that vary in $[0,\pi]$, $[0,2\pi]$ ranges respectively.

Hence, the following article has been divided into various sections for better understanding. Section (2) mentions about the general scalar tensor theory and the field equations, along with some physical quantities. Section (3) mainly deals with the physical and geometrical properties of the cosmological model that are ascertained with the help of corresponding graphs w.r.t $'z'$ (where z is the redshift defined through $1+z=\frac{a_0}{a_1}$ setting the current value of the scale factor to $a_0 = 1$). In the last section the obtained results have been concluded.

2. FIELD EQUATIONS FOR GENERAL SCALAR-TENSOR THEORY

Nordtvedt [57] has suggested the scalar tensor gravitational theories of a general class, where the Brans-Dicke theory parameter ω is an arbitrary (positive definite) function of the scalar field as $\omega \rightarrow \omega(\varphi)$. Schwinger [58] has attracted a lot of work by considering a specific case of Nordtvedt's theory to evaluate the scalar field cosmological models. Also, the theories of Jordan [59] and, Brans and Dicke [60] have been taken as a special case in the general class of scalar-tensor gravitational theories. This theory has been considered by some of the researchers [61–64] to understand the Universe. Higher-derivative operators and effective field theory for general scalar-tensor theories have been considered by Solomon and Trodden [65]. Huang et al. [66], have analyzed the stability of Einstein static Universes in general scalar–tensor theory with non-minimal derivative coupling by analyzing scalar and tensor perturbations. Also, much recently a simplified approach to general scalar-tensor theories has been made by Bloomfield [67]. López et al. [68] have studied a chaotic inflation and reheating in generalized scalar-tensor gravity.

The proposed field equations by Nordtvedt are given by,

$$R_{\mu\nu}-\frac{1}{2}g_{\mu\nu}R=-8\pi\phi^{-1}T_{\mu\nu}-\omega\phi^{-2}(\phi_{,\mu}\phi_{,\nu}-\frac{1}{2}g_{\mu\nu}\phi_{,k}\phi^{,k})-\phi^{-1}(\phi_{\mu;\nu}-g_{\mu\nu}\phi^{;k}_{;k}), \tag{4}$$

$$\phi^{;k}_{;k}=\frac{1}{3+2\omega}\left(8\pi T-\frac{d\omega}{d\phi}\phi_{,\mu}\phi^{,\mu}\right), \tag{5}$$

where $R_{\mu\nu}$ & R is the Ricci tensor and scalar curvature respectively; and $T_{\mu\nu}$ is the stress energy tensor of the matter, T is the trace of $T_{\mu\nu}$ and comma and semicolon represent the partial and covarient differentiation respectively. Also, from field Eqs. (4) and (5) we get the conservation equation is given as,

$$T^{\mu\nu}{}_{;\mu}=0. \tag{6}$$

The DE and pressureless matter combinedly constitutes the cosmos, which can be defined as,

$$T_{\mu\nu}=\rho_m u_\mu u_\nu, \tag{7}$$

$$\&\quad \bar{T}_{\mu\nu}=(\rho_{de}+p_{de})u_\mu u_\nu-p_{de}g_{\mu\nu}, \tag{8}$$

where p_{de} is the pressure of RHDE; whereas, ρ_m and ρ_{de} are the matter energy density and the energy density of RHDE. The presumption of taking the anisotropic DE, whose energy–momentum tensor, $T_{\mu\nu}$ as given below, determines the study of present cosmic accelerated expansion,

$$\bar{T}_{\mu\nu}=[1,-\omega_r,-\omega_\theta,-\omega_\phi]\rho_{de}=[1,-\omega_{de},-\omega_{de},-\omega_{de}]\rho_{de}, \tag{9}$$

where the directional EoS parameters: $\omega_r=-\omega_{de}$, $\omega_\theta=-\omega_{de}$ and $\omega_\phi=-\omega_{de}$ are along r, θ and ϕ respectively.

Hence, we obtain the following field equations from the equations (4), (5) and (9) as follows:

$$\frac{2\ddot{B}}{B}+\frac{\dot{B}^2}{B^2}+\frac{1}{B^2}-\frac{\omega\dot{\phi}^2}{2\phi^2}-\frac{\ddot{\phi}}{\phi}-\frac{2\dot{B}\dot{\phi}}{B\phi}=-\frac{8\pi\omega_{de}\rho_{de}}{\phi}, \tag{10}$$

$$\frac{\ddot{A}}{A}+\frac{\ddot{B}}{B}+\frac{\dot{A}\dot{B}}{AB}-\frac{\omega\dot{\phi}^2}{2\phi^2}-\frac{\ddot{\phi}}{\phi}-\frac{\dot{\phi}}{\phi}\left(\frac{\dot{A}}{A}+\frac{\dot{B}}{B}\right)=-\frac{8\pi\omega_{de}\rho_{de}}{\phi}, \tag{11}$$

$$2\frac{\dot{A}\dot{B}}{AB}+\frac{\dot{B}^2}{B^2}+\frac{1}{B^2}+\frac{\omega\dot{\phi}^2}{2\phi^2}-\frac{\dot{\phi}}{\phi}\left(\frac{\dot{A}}{A}+\frac{2\dot{B}}{B}\right)=-\frac{8\pi(\rho_m+\rho_{de})}{\phi}, \tag{12}$$

$$\&\quad \ddot{\phi}+\dot{\phi}\left(\frac{\dot{A}}{A}+\frac{2\dot{B}}{B}\right)=\frac{8\pi\left[3\omega_{de}\rho_{de}-\rho_m-\rho_{de}\right]}{3+2\omega}-\frac{1}{3+2\omega}\frac{d\omega}{d\phi}\dot{\phi}^2. \tag{13}$$

The transformation $dt=AB^2d\tau$, can be used to rewrite the above field equations (10)-(13) as,

$$\frac{1}{A^2B^4}\left[\frac{2B''}{B}-\frac{3B'^2}{B^2}-\frac{2A'B'}{AB}+A^2B^2-\frac{\omega\phi'^2}{2\phi^2}-\frac{\phi''}{\phi}+\frac{A'\phi'}{A\phi}\right]=\frac{-8\pi\omega_{de}\rho_{de}}{\phi}, \tag{14}$$

$$\frac{1}{A^2B^4}\left[\frac{A''}{A}+\frac{B''}{B}-\frac{A'^2}{A^2}-\frac{2B'^2}{B^2}-\frac{2A'B'}{AB}-\frac{\omega\phi'^2}{2\phi^2}-\frac{\phi''}{\phi}+\frac{B'\phi'}{B\phi}\right]=\frac{-8\pi\omega_{de}\rho_{de}}{\phi}, \tag{15}$$

$$\frac{1}{A^2B^4}\left[\frac{2A'B'}{AB}+\frac{B'^2}{B^2}+A^2B^2+\frac{\omega\phi'^2}{2\phi^2}-\frac{\phi'}{\phi}\left(\frac{A'}{A}+\frac{2B'}{B}\right)\right]=-\frac{8\pi(\rho_{de}+\rho_m)}{\phi}, \tag{16}$$

$$\& \quad (3+2\omega)\phi''=8\pi\left[3\omega_{de}\rho_{de}-\rho_m-\rho_{de}\right](A^2B^4)-\frac{d\omega}{d\phi}\phi'^2. \tag{17}$$

Here the overhead dot (.) denotes differentiation w.r.t 't', the overhead dash ($'$) denotes differentiation w.r.t τ and the field equations (14)-(17) corresponds to KS-Universe.
Therefore, from equations (14)-(17), we have obtained,

$$(3+2\omega)\phi''+\frac{d\omega}{d\phi}\phi'^2=2\phi\left[\frac{A''}{A}-\frac{A'^2}{A^2}-\frac{2A'B'}{AB}+\frac{2B''}{B}-\frac{3B'}{B}+A^2B^2\right]+3\phi''+\frac{\omega\phi'^2}{\phi^2}. \tag{18}$$

There are four field equations (14)-(17) and six unknowns - A, B, ϕ, ρ_{de}, ρ_m and ω_{de} that are to be determined. As a specific case proposed by Schwinger [58] in the following form,

$$3+2\omega(\phi)=\frac{1}{\lambda\phi}, \quad \lambda\text{= constant}, \tag{19}$$

we have obtained Nordtvedt's general scalar tensor cosmic model in the framework of RHDE.

Hence, from equations (18) and (19) we obtain,

$$\frac{1}{\lambda}\left[\frac{\phi''}{\phi}-\frac{\phi'^2}{\phi^2}\right]+\frac{3\phi'^2}{2\lambda\phi}-3\phi''=2\phi\left[\frac{A''}{A}-\frac{A'^2}{A^2}-\frac{2A'B'}{AB}+\frac{2B''}{B}-\frac{3B'^2}{B^2}+A^2B^2\right]. \tag{20}$$

The preceding equation has been solved by the condition of proportionality between the shear scalar and the expansion scalar as,

$$A=B^n, \quad n>1. \tag{21}$$

From equations (20) and (21) we get,,

$$\phi=e^{k_1\tau+k_2}, \tag{22}$$

$$\text{and} \quad \frac{B''}{B}-\frac{3(n+1)}{n+2}\frac{B'^2}{B^2}=-\frac{1}{n+2}B^{n+2}-\frac{3}{n+2}k_1^2, \tag{23}$$

where k_1 and k_2 represent the arbitrary constants. And, on solving equation (23) we obtain the metric potentials as:

$$A=\left(\frac{\beta_1}{\beta_2}\operatorname{sech}\left(\beta_1(n+1)\tau\right)\right)^{\frac{n}{n+1}}, \tag{24}$$

$$B=\left(\frac{\beta_1}{\beta_2}\operatorname{sech}\left(\beta_1(n+1)\tau\right)\right)^{\frac{1}{n+1}}. \tag{25}$$

Firstly, we have studied various physical parameters, like volume (V), scale factor ($a(t)$), Hubble parameter (H), expansion scalar (ϑ), shear scalar (σ^2) and the anisotropic parameter ($\mathcal{A}_h$) whose expressions are given respectively as,

$$V=\left(\frac{\beta_1}{\beta_2}\operatorname{sech}\left(\beta_1(n+1)\tau\right)\right)^{\frac{n+2}{n+1}}, \tag{26}$$

$$a=\left(\frac{\beta_1}{\beta_2}\operatorname{sech}\left(\beta_1(n+1)\tau\right)\right)^{\frac{n+2}{3n+3}}, \tag{27}$$

$$H=\frac{-(n+2)\beta_1\tanh\left(\beta_1(n+1)\tau\right)}{3}, \tag{28}$$

$$\vartheta=-(n+2)\beta_1\tanh\left(\beta_1(n+1)\tau\right), \tag{29}$$

$$\sigma^2=\frac{(n-1)^2\beta_1^2\tanh^2\left(\beta_1(n+1)\tau\right)}{3}, \tag{30}$$

$$\& \quad \mathcal{A}_h=\frac{2(n-1)^2}{(n+2)^2}. \tag{31}$$

For the RHDE, the energy density takes the value,

$$\rho_{de} = \frac{d^2\beta_1^4 \sinh^4\left(\beta_1(n+1)\tau\right)(n+2)^4}{3\left(\left((n+2)^2\beta_1^2 + 9\pi\delta\right)\cosh^2\left(\beta_1(n+1)\tau\right) - (n+2)^2\beta_1^2\right)\cosh^2\left(\beta_1(n+1)\tau\right)}, \tag{32}$$

and the energy density of matter has the following expression

$$\left.\begin{aligned}\rho_m =& \frac{e^{\tau k_1 + k_2}}{8\pi}\left(\frac{\beta_1}{\beta_2}\operatorname{sech}\left(\beta_1(n+1)\tau\right)\right)^{\frac{-2n-4}{n+1}} \frac{\operatorname{sech}^2\left(\beta_1(n+1)\tau\right)}{2\beta_2^2}\Bigg(-4\times \\ &\left((n+\frac{1}{2})\beta_1^2 - \frac{\omega k_1^2}{4}\right)\beta_2^2\cosh^2\left(\beta_1(n+1)\tau\right) + 2k_1\beta_1\beta_2^2(n+2)\times \\ &\sinh\left(\beta_1(n+1)\tau\right)\cosh\left(\beta_1(n+1)\tau\right) + 4\beta_1^2\left(\frac{-1}{2} + (n+\frac{1}{2})\beta_2^2\right)\Bigg) - \rho_{de}\end{aligned}\right\} \tag{33}$$

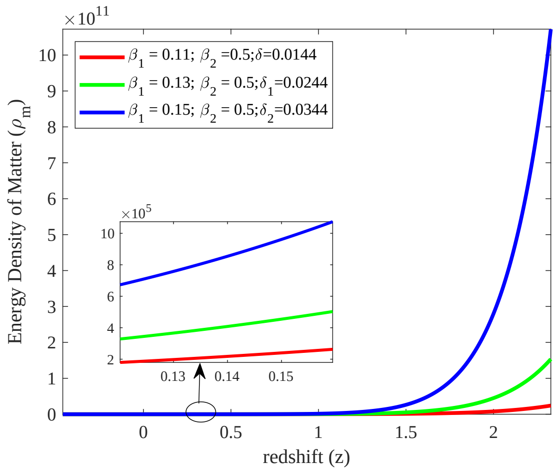

Figure 1. Illustration of energy density matter (ρ_m) against redshift (z)

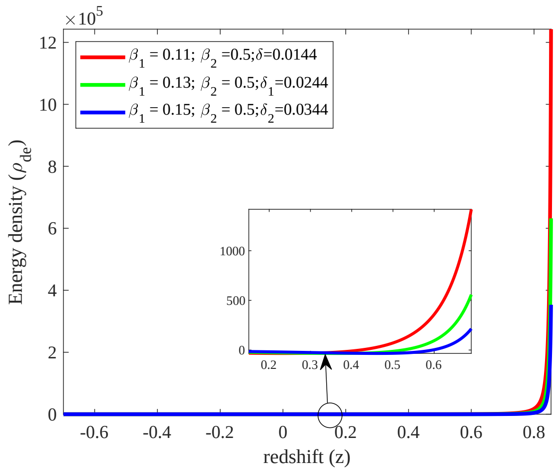

Figure 2. Illustration of energy density of DE (ρ_{de}) against redshift (z)

Thus, Eq. (3) becomes,

$$ds^2 = -dt^2 + \left(\frac{\beta_1}{\beta_2}\operatorname{sech}\left(\beta_1(n+1)\tau\right)\right)^{\frac{2n}{n+1}} dr^2 + \left(\frac{\beta_1}{\beta_2}\operatorname{sech}\left(\beta_1(n+1)\tau\right)\right)^{\frac{2}{n+1}} (d\theta^2 + \sin^2\theta d\varphi^2). \tag{34}$$

For various β_1, β_2 and δ values, the energy density of matter (ρ_m) and RHDE (ρ_{de}) have been constructed against redshift (z) in Figs. (1) and (2) respectively. It can be seen from their graphical course that the trajectories vary in positive region decreasing against redshift (z), which indicates rapid cosmic expansion. From the equation (26) it can be noticed that, at initial periods of the cosmos formation i.e., at $\tau = 0$, the volume (V) and scale factor (a) of the Universe is constant, but as time $\tau \longrightarrow \infty$ the Universe has been expanding i.e., $V \longrightarrow \infty$. Also, from equations (28)-(30), we can categorically say that, at the initial time phase ($\tau = 0$), all the parameters H, ϑ and σ vanish and as τ increases these parameters increase, illustrating an inflationary scenario of the Universe, expanding at a constant rate. From equation (31), we observe that $\mathcal{A}_h \neq 0$ throughout the evolution of the Universe, and our model (34) is an anisotropic model.

3. PHYSICAL AND GEOMETRICAL INTERPRETATIONS OF THE MODEL

The parameters such as EoS (ω_{de}), EoS plane ($\omega_{de} - \omega'_{de}$), deceleration parameter (q), stability (v_s^2), density (Ω_{de}), jerk (j), Om(z) and statefinder ($r - s$) have been studied in this particular section to understand the constructed model of the Universe in a better way.

- **Equation of state parameter (ω_{de}):** Study of the Universe has always been a mysterious task, and with the mysterious component, so called the DE, it has been more difficult to understand the nature of the cosmos. However, the EoS parameter might help us to evaluate the nature of the Universe to some extent. ω_{de} is used to study the acceleration of the cosmos and the phase change from deceleration to acceleration, and is defined as,

$$\omega_{de} = \frac{p_{de}}{\rho_{de}}. \tag{35}$$

For the model, we get the EoS parameter as

$$\omega_{de} = \frac{3\Psi_1}{8\pi d^2 \beta_2^2 \beta_1^4 \sinh^4\left(\beta_1 (n+1)\tau\right)\left(n+2\right)^4}, \tag{36}$$

$$\text{where} \quad \Psi_1 = \left(\frac{\beta_1}{\beta_2}\,\text{sech}\left(\beta_1(n+1)\tau\right)\right)^{\frac{-2n-4}{n+1}} \left(\left((n^2-4n-2)\beta_1^2 + \frac{k_1^2}{2}(4+\omega)\right)\times \beta_2^2 \cosh^2\left(\beta_1(n+1)\tau\right) + \beta_1\beta_2^2((k_1+1)n+k_1)\sinh\left(\beta_1(n+1)\tau\right)\times \cosh\left(\beta_1(n+1)\tau\right) - 2\beta_1^2\left(\frac{-1}{2} + (n^2+\frac{1}{2})\beta_2^2\right)\right) e^{\tau k_1 + k_2}\left(\left((n+2)^2\times \beta_1^2 + 9\pi\delta\right)\cosh^2\left(\beta_1(n+1)\tau\right) - (n+2)^2\beta_1^2\right).$$

The EoS (ω_{de}) parameter has been plotted against redshift (z), for different values of δ. It is observed from Fig. (3), the model starts its evolution from the quintessence region as ω_{de} lies in the range $(-1, 1/3)$, then crosses the phantom divide line at $\omega_{de} = -1$ behaving like a non-relativistic matter, and finally reaches the phantom region, as $\omega_{de} < -1$. Such a behavior of the model is called as quintessence like nature.

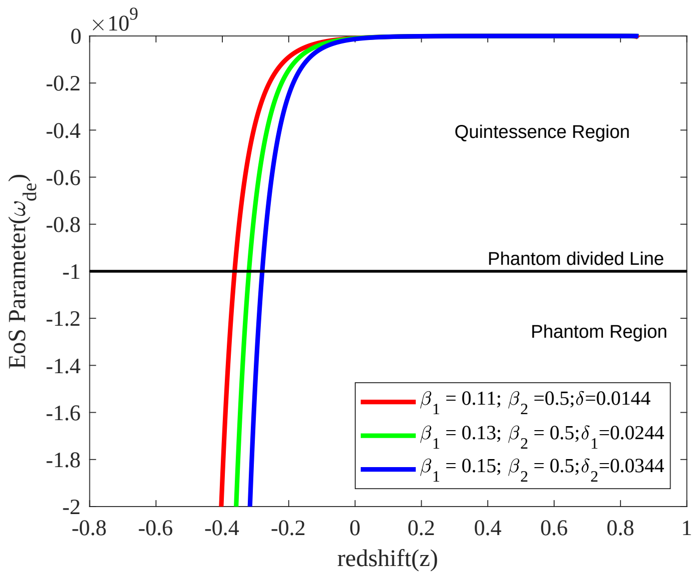

Figure 3. Illustration of EoS parameter (ω_{de}) against redshift (z)

- **EoS plane ($\omega_{de} - \omega'_{de}$):** As proposed by Cadwell and Linder [69] the $\omega_{de} - \omega'_{de}$ plane describes the various regions of Universe's expansion which evaluates the quintessence scalar field. For the values of ω_{de} and ω'_{de}, such as $\omega_{de} < 0$, $\omega'_{de} > 0$ and $\omega_{de} < 0$, $\omega'_{de} < 0$ the EoS plane is characterized into thawing region and freezing region respectively. The EoS plane for the model is given by,

$$\omega'_{de} = \frac{-9\Psi_2}{4\beta_2^2(n+2)^5\beta_1^5 \sinh^6\left(\beta_1(n+1)\tau\right)\pi d^2}, \tag{37}$$

$$
\begin{aligned}
\text{where}\quad \Psi_2 = &\Big(\beta_1\Big((n^3-2n^2-10n-4)\beta_1^2+\frac{k_1}{2}\Big(\Big(1+(\omega+5)k_1\Big)n+k_1(2\omega+9)\Big)\Big)\times\\
&\Big((n+2)^2\beta_1^2+9\pi\delta\Big)\beta_2^2\cosh^6\left(\beta_1(n+1)\tau\right)+\frac{3}{2}\Big(\Big((k_1+\frac{2}{3})n^2+\Big(\frac{2k_1}{3}\\
&+\frac{4}{3}\Big)n+\frac{7k_1}{3}\Big)\beta_1^2+\frac{k_1^3}{6}(4+\omega)\Big)\Big((n+2)^2\beta_1^2+9\pi\delta\Big)\beta_2^2\sinh\left(\beta_1(n+1)\tau\right)\times\\
&\cosh^5\left(\beta_1(n+1)\tau\right)-3\Big((n+2)^2\Big(\frac{-1}{3}+\Big(n^3-\frac{5n^2}{3}-\frac{26n}{3}-3\Big)\beta_2^2\Big)\beta_1^4\\
&+\Big(\Big(\Big((\frac{\omega}{2}+\frac{7}{3})k_1^2+\frac{k_1}{3}+9\pi\delta\Big)n^3+\Big((\frac{17\omega}{6}+13)k_1^2+\frac{4k_1}{3}-18\pi\delta\Big)n^2\\
&+\Big((\frac{16\omega}{3}+24)k_1^2+\frac{4k_1}{3}-66\pi\delta\Big)n+(\frac{44}{3}+\frac{10\omega}{3})k_1^2-21\pi\delta\Big)\beta_2^2-3\pi\delta\Big)\beta_1^2\\
&+\frac{9\pi\delta}{2}\Big(\Big(\frac{1}{3}+(\omega+\frac{13}{3})k_1\Big)n+\frac{4}{3}(\omega+\frac{17}{4})k_1\Big)\beta_2^2\delta k_1\Big)\beta_1\cosh^4\left(\beta_1(n+1)\tau\right)\\
&-4\beta_1^2\Big(\Big(\Big((k_1+\frac{5}{8})n^2+\Big(\frac{5k_1}{4}+\frac{9}{8}\Big)n+k_1\Big)\beta_2^2-\frac{k_1}{8}\Big)(n+2)^2\beta_1^2+\Big(\Big((\frac{\omega}{16}+\frac{1}{4})k_1^3\\
&+\frac{63\pi\delta k_1}{8}+\frac{45\pi\delta}{8}\Big)n^2+\Big((\frac{\omega}{4}+1)k_1^3+\frac{27\pi\delta k_1}{2}+\frac{63\pi\delta}{8}\Big)n+\Big(\frac{\omega}{4}+1\Big)k_1^3+9\pi\delta k_1\Big)\beta_2^2\\
&-\frac{9\pi\delta k_1}{8}\Big)\sinh\left(\beta_1(n+1)\tau\right)\cosh^3\left(\beta_1(n+1)\tau\right)+4\beta_1^3\Big((n+2)^2\Big(\Big(n^3+\frac{n^2}{4}-\frac{15n}{4}\\
&-\frac{3}{4}\Big)\beta_2^2-\frac{n}{4}-\frac{3}{4}\beta_1^2+\Big(\Big((\frac{9}{8}+\frac{\omega}{4})k_1^2+\frac{k_1}{8}+9\pi\delta\Big)n^3+\Big(\Big(\frac{49}{8}+\frac{11\omega}{8}\Big)k_1^2+\frac{k_1}{2}\\
&+\frac{27\pi\delta}{2}\Big)n^2+\Big(\Big(11+\frac{5\omega}{2}\Big)k_1^2+\frac{k_1}{2}+\frac{9\pi\delta}{2}\Big)n+\Big(\frac{3\omega}{2}+\frac{13}{2}\Big)k_1^2+\frac{27\pi\delta}{4}\Big)\beta_2^2\\
&-\frac{9\pi}{2}(n+\frac{3}{2})\delta\Big)\cosh^2\left(\beta_1(n+1)\tau\right)+\frac{5}{2}\beta_1^4(n+2)^2\Big(\Big((k_1+\frac{3}{5})n^2+(\frac{8k_1}{5}+1)n\\
&+\frac{6k_1}{5}\Big)\beta_2^2-\frac{k_1}{5}\Big)\sinh\left(\beta_1(n+1)\tau\right)\cosh\left(\beta_1(n+1)\tau\right)-2\beta_1^5(n+2)^3\Big(\frac{-1}{2}\\
&+(n^2+\frac{1}{2})\beta_2^2\Big)\Big)\Big(\frac{\beta_1}{\beta_2}\operatorname{sech}\left(\beta_1(n+1)\tau\right)\Big)^{\frac{-2n-4}{n+1}}e^{k_1\tau+k_2}\Big).
\end{aligned}
$$

As depicted from the Fig. (4), $\omega_{de}-\omega'_{de}$ plane has been taken against redshift (z) for different values of δ. Here, the trajectories varies in the negative region, characterizing the freezing region as $\omega_{de}<0$ and $\omega'_{de}<0$. These observations are in correspondence with the recent observations.

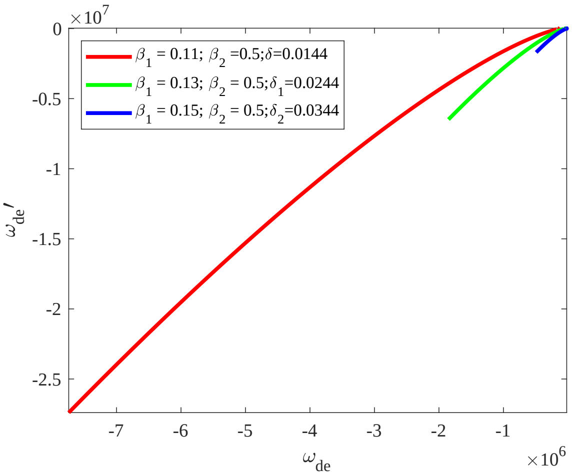

Figure 4. Illustration of EoS plane

- **Deceleration Parameter (q):** The deceleration parameter (q), more explicitly, the signature of q determines the nature of accelerating expansion of the cosmos. Whenever, $q > 0$ the Universe shows decelerating expansion and when $q < 0$ there is rapid expansion of the cosmos. Here, the deceleration parameter (q) is defined as,

$$q = -1 + \frac{d}{dt}\left(\frac{1}{H(t)}\right). \tag{38}$$

The deceleration parameter for our model is given by,

$$q = \frac{(-n-2)\cosh^2\left(\beta_1(n+1)\tau\right) + 4n + 5}{(n+2)\sinh^2\left(\beta_1(n+1)\tau\right)}. \tag{39}$$

Therefore, we can observe from the Fig. (5) that deceleration parameter (q) has been constructed against redshift (z) for distinct estimates of β_1 and β_2. The trajectories of q projects that the Universe travels previously from decelerated phases to the current accelerating phase. The model basically shows exponential or the de-Sitter expansion, as it is observed that $q = -1$.

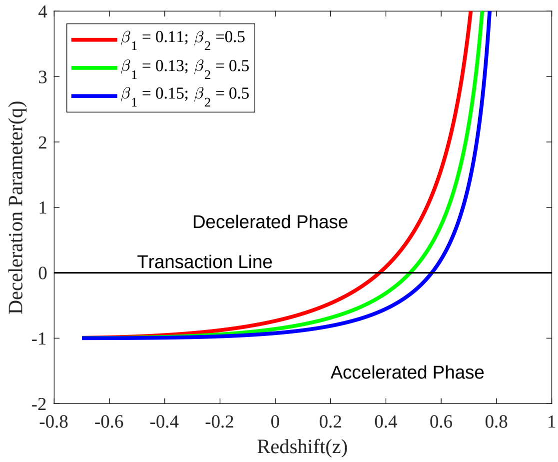

Figure 5. Illustration of deceleration parameter (q) against redshift (z)

- **Analysis of Model's Stability:** The squared speed of sound has a vital role in analyzing the stability of any model. The model exhibits a stable behavior whenever $v_s^2 > 0$ and shows an unstable behavior when $v_s^2 < 0$. The model's stability can be determined with the help of following mathematical formula:

$$v_s^2 = \frac{\dot{p}_{de}}{\dot{\rho}_{de}}. \tag{40}$$

The squared speed of the sound for the obtained model is given by,

$$v_s^2 = \frac{\Psi_3}{\Psi_4}, \tag{41}$$

$$\left.\begin{aligned}
\text{where}\quad \Psi_3 =& \frac{9}{16}\left(\left(\frac{\beta_1}{\beta_2}\operatorname{sech}\left(\beta_1(n+1)\tau\right)\right)^{\frac{-2n-4}{n+1}} e^{k_1\tau+k_2}\left(\left((n+2)^2\beta_1^2 + 9\pi\delta\right)\cosh^2\left(\beta_1(n+1)\tau\right)\right.\right.\\
&-(n+2)^2\beta_1^2\Big)^2\left(\left(\left(\left((k_1+\frac{2}{3})n^2 + \left(\frac{2k_1}{3}+\frac{4}{3}\right)n + \frac{2k_1}{3}\right)\beta_1^2 + \frac{k_1^3(4+\omega)}{6}\right)\beta_2^2\times\right.\right.\\
&\cosh^3\left(\beta_1(n+1)\tau\right) + \frac{2}{3}\left((n^3-2n^2-10n-4)\beta_1^2 + \frac{k_1}{2}\left(\left(1+(\omega+5)k_1\right)n\right.\right.\\
&\left.\left.+k_1(2\omega+9)\right)\right)\beta_1\beta_2^2\sinh\left(\beta_1(n+1)\tau\right)\cosh^2\left(\beta_1(n+1)\tau\right) - \beta_1^2\left(\left((k_1+\frac{1}{3})n^2\right.\right.\\
&\left.+(\frac{4k_1}{3}+1)n + \frac{4k_1}{3}\right)\beta_2^2 - \frac{k_1}{3}\Big)\cosh\left(\beta_1(n+1)\tau\right) - \frac{4}{3}\left(\frac{-1}{2}+(n^2+\frac{1}{2})\right)\beta_2^2\Big)\times\\
&\beta_1^3\sinh\left(\beta_1(n+1)\tau\right)\Big),
\end{aligned}\right\}$$

$$\text{and}\quad \Psi_4 = \left(\pi\left(\left((n+2)^2\beta_1^2 + 18\pi\delta\right)\cosh^2\left(\beta_1(n+1)\tau\right) - (n+2)^2\beta_1^2\right)d^2\beta_1^5(n+1)\beta_2^2(n+2)^4\sinh^3\left(\beta_1(n+1)\tau\right)\right).\Bigg\}$$

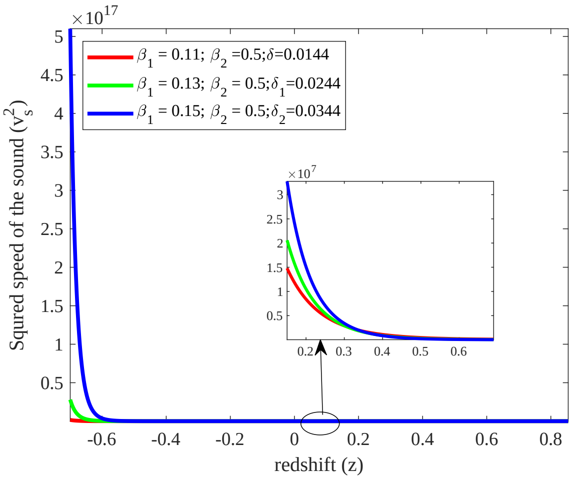

Figure 6. Squared speed of sound (v_s^2) against redshift (z)

From the Fig. (6) it is observed that v_s^2 is plotted against z to understand the model's stability. Here, trajectories are completely varying positive region for several values of δ. This illustrates Universe's stable behavior.

- **Density Parameter:** For a DE model, the density parameter has been defined as

$$\Omega_{de} = \frac{\rho_{de}}{3H^2}.$$

The density parameter for our model is obtained as,

$$\Omega_{de} = \frac{d^2\beta_1^2\sinh^2\left(\beta_1(n+1)\tau\right)(n+2)^2}{\left((n+2)^2\beta_1^2 + 9\pi\delta\right)\cosh^2\left(\beta_1(n+1)\tau\right) - (n+2)^2\beta_1^2}. \tag{42}$$

In order to analyze the behavior of the density parameter Ω_{de} we have the graphical representation of Ω_{de} against redshift (z) for various values of δ in the Fig. (7). It can be observed that the trajectories are varying in the positive region, decreasing against redshift.

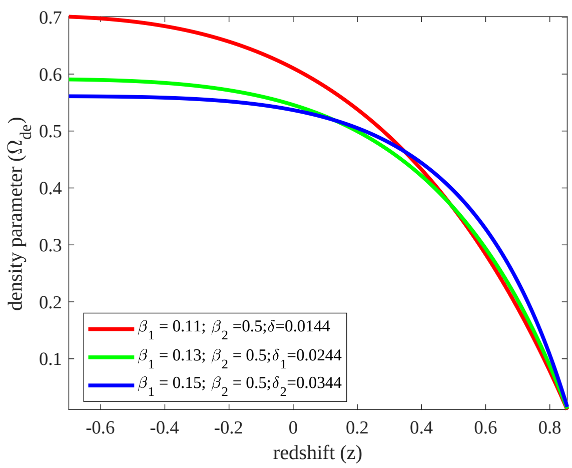

Figure 7. Illustration of density parameter (Ω_{de}) against redshift (z)

- **Jerk Parameter (j):** In an cosmic evolution, the jerk parameter is defined as,

$$j = \frac{\dddot{a}}{aH^3}, \tag{43}$$

where a and H are the cosmic scale factor and the Hubble parameter. Here, the scale factor has been differentiated w.r.t. the cosmic time. The jerk parameter (j) happens to be the 4^{th} expression of a_0 in a Taylor series expansion:

$$\frac{a(t)}{a_0} = 1 + H_0(t-t_0) - \frac{1}{2}q_0H_0^2(t-t_0)^2 + \frac{1}{6}j_0H_0^3(t-t_0)^3 + O[(t-t_0)^4], \tag{44}$$

where a_0 denotes the present value. The jerk parameter for our model is obtained as,

$$j = \frac{(n+2)^2\cosh^2\left(\beta_1(n+1)\tau\right) - 28n^2 - 67n - 40}{\sinh^2\left(\beta_1(n+1)\tau\right)(n+2)^2}. \tag{45}$$

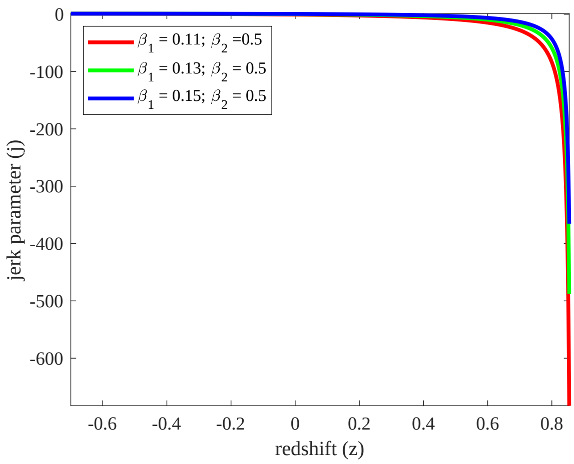

Figure 8. Illustration of jerk parameter (j) against redshift (z)

Fig. (8) depicts the construction of jerk parameter (j) against redshift (z). It is clearly observed that the curves of j are completely varying in the negative region for all the values of β_1 and β_2 and approaches to unity in late times.

- **Om(z)- diagnostic:** Om-diagnostics is an another tool discovered by Sahni et al. [70] other than statefinder plane, to differentiate the various phases of the Universe. A positive path of the curve indicates that the model corresponds to phantom DE and the path of the curve oriented in the negative region indicates a quintessence DE. The Om(z) in terms of $H(z)$ function is defined as,

$$Om(z) = \frac{H^2(z) - H_0^2}{H_0^2[(1+z)^3 - 1]}, \tag{46}$$

where,

$$H(z) = \frac{-\beta_1(n+2)}{3}\sqrt{1 - \frac{\beta_2^2}{\beta_1^2}\left(\frac{a_0}{1+z}\right)^{\frac{6n+6}{n+2}}}. \tag{47}$$

We can depict that in the Fig. (9) the path of the Om(z), as taken against redshift(z) differs in negative region, thus having a quintessence behavior.

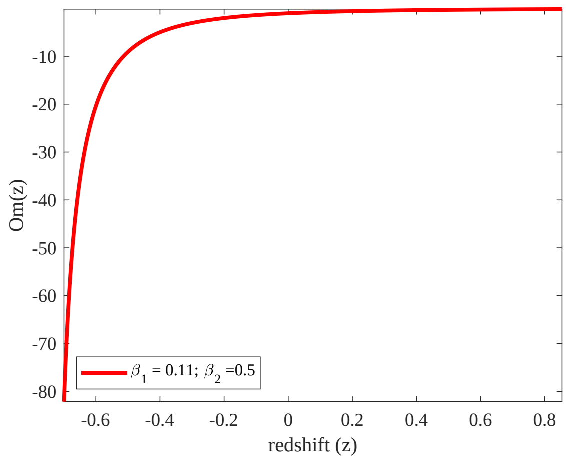

Figure 9. Illustration of Om(z) against redshift (z)

- **Statefinder Pair (r,s):** The study and discrimination of essential DE models can be done with a sensitive and a geometrical diagnostic pair- (r,s) that had been developed by Sahni et al. [71] and Alam et al. [72]. This helps us to understand the process of Universe's acceleration. The statefinder pair (r,s) that purely depends on scale factor (a) and is defined as

$$r=\frac{\dddot{a}}{aH^3}\quad \&\quad s=\frac{r-1}{3(q-1/2)}.$$

For the constructed model, we have

$$r=\frac{(n+2)^2\cosh^2\left(\beta_1(n+1)\tau\right)-28n^2-67n-40}{\sinh^2\left(\beta_1(n+1)\tau\right)(n+2)^2}, \tag{48}$$

$$\&\quad s=\frac{1}{(n+2)^3\sinh\left(\beta_1(n+1)\tau\right)^4}\left\{\begin{aligned}&\Big((n+2)^3\cosh\left(\beta_1(n+1)\tau\right)^4+\big(-200n^3-714n^2\\&-852n-340\big)\cosh\left(\beta_1(n+1)\tau\right)^2+280n^3+978n^2+1137n+440\Big).\end{aligned}\right.$$

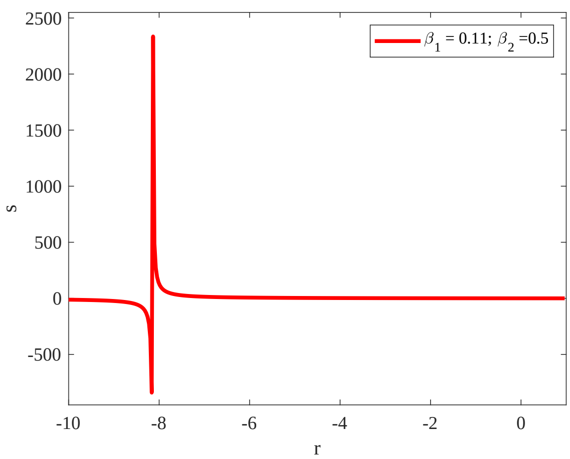

Figure 10. Illustration of $r-s$ plane

From the Fig. (10), which is the construction of $r-s$ plane, it can be interpreted that, the Universe begins its evolution from the quintessence and phantom region and finally reaches the ΛCDM region for $r=1$, $s=0$.

4. CONCLUSIONS

It has been many decades by now, that the scientists have started the process of figuring out the puzzling component: the DE and finding out the causes for the accelerated expansion of the cosmos. In such an attempt, we have built a model that helps us to understand these things. The constructed model describes the KS-Universe in the backdrop of RHDE in a general scalar tensor theory. It is observed that the Universe is homogeneous and anisotropic with a continuous expansion. Because of positive and decreasing energy density of matter (ρ_m) and as well as DE (ρ_{de}), the cosmos shows a rapid expansion. Also, a quintessence nature of the space is projected by the EoS parameter (ω_{de}); and the Universe is mainly characterized by freezing region, as $\omega_{de} < 0$ and $\omega'_{de} < 0$. The deceleration parameter (q) suggests that the Universe has a transition from erstwhile deceleration to present acceleration and shows a de-Sitter expansion at $q = -1$. The stability of the model has been examined with the help of squared speed of sound, which describes a stable behavior for the cosmos. The density parameter (Ω_{de}) varies in the positive region, decreasing against redshift (z) and where as the jerk parameter (j) approaches to unity as the time passes, while differing in the negative region. The Om(z) parameter depicts the quintessence behavior of the cosmos, as the parameter is varying in the negative region. And, finally the statefinder plane ($r-s$) evolves from quintessence and phantom region and reaches the ΛCDM region for $r = 1$ and $s = 0$. Our observations are in concurrent with the recent studies and various experiments, and thus holding the sustainability of the model.

Acknowledgments

MVS acknowledges Department of Science and Technology (DST), Govt of India, New Delhi for financial support to carry out the Research Project [No. EEQ/2021/000737, Dt. 07/03/2022].

ORCID

T. Chinnappalanaidu, https://orcid.org/0000-0001-6902-2820; **S. Srivani Madhu**, https://orcid.org/0009-0002-2640-3011; **M. Vijaya Santhi**, https://orcid.org/0000-0002-0050-3033; **N. Sri Lakshmi Sudha Rani**, https://orcid.org/0009-0009-9593-954X; **A. Krishna Rao**, https://orcid.org/0000-0003-2786-9526

REFERENCES

[1] I. Bars, and J. Terning, *Extra Dimensions in Space and Time*, (Springer, NY, 2010). https://doi.org/10.1007/978-0-387-77638-5
[2] P.A.R. Ade, *et al*., Astronomy & Astrophysics, **571**, A16 (2014). https://doi.org/10.1051/0004-6361/201321591
[3] S. Perlmutter, *et al*., Astrophys. J. **517**, 565 (1999). https://doi.org/10.1086/307221
[4] A.G. Riess, *et al*., Astron. J. **116**, 1009 (1998). https://doi.org/10.1086/300499
[5] F. Zwicky, Astrophys. J. **83**, 23 (1936). https://doi.org/10.1086/143697
[6] F. Zwicky, Astrophys. J. **86**, 217 (1937). https://doi.org/10.1086/143864
[7] V.C. Rubin, and W.K. Ford, Astrophys. J. **159**, 379 (1970). https://doi.org/10.1086/150317
[8] R.V. Marttens, *et al*., Phys. Dark Uni. **28**, 100490 (2020). https://doi.org/10.1016/j.dark.2020.100490
[9] N. Aghanim, *et al*., Astro. Astrophys. **641**, A6 (2020). https://doi.org/10.1051/0004-6361/201833910
[10] S. Alam, *et al*., Astronomical Society, **470**, 2617 (2017). https://doi.org/10.1093/mnras/stx721
[11] P. Horava, and D. Minic, Phys. Rev.Lett. **85**, 1610 (2000). https://doi.org/10.1103/PhysRevLett.85.1610
[12] S.D. Thomas, Phys. Rev. Lett. **89**, 081301 (2002). https://doi.org/10.1103/PhysRevLett.89.081301
[13] S.D.H. Hsu, Phys. Lett. B, **594**, 13 (2004). https://doi.org/10.1016/j.physletb.2004.05.020
[14] S. Wang, *et al*., Phys. repo. **696**, 1 (2017). https://doi.org/10.1016/j.physrep.2017.06.003
[15] A.G. Cohen, *et al*., Phys. Rev. Lett. **82**, 4971 (1999). https://doi.org/10.1103/PhysRevLett.82.4971
[16] B. Guberina, *et al*., J. Cosm. Astro. Phys. **2007**, 012 (2007). https://doi.org/10.1088/1475-7516/2007/01/012
[17] L. Susskind, J. Math.Phys. **36**, 6377 (1995). https://doi.org/10.1063/1.531249
[18] M. Li, Phys. Lett. B, **603**, 1 (2004). https://doi.org/10.1016/j.physletb.2004.10.014
[19] S. Nojiri, and S.D. Odintsov, Gen. Rel. Grav. **38**, 1285 (2006). https://doi.org/10.1007/s10714-006-0301-6
[20] S. Nojiri, and S.D. Odintsov, Eur. Phys. J. C, **77**, 528 (2017). https://doi.org/10.1140/epjc/s10052-017-5097-x
[21] A.S. Jahromi, *et al*., Phys. Lett. B, **780**, 21 (2018). https://doi.org/10.1016/j.physletb.2018.02.052
[22] C. Tsallis, and L.J.L. Cirto, Eur. Phys. J. C, **73**, 2487 (2013). https://doi.org/10.1140/epjc/s10052-013-2487-6
[23] H. Moradpour, *et al*., Eur. Phys. J. C, **78**, 829 (2018). https://doi.org/10.1140/epjc/s10052-018-6309-8
[24] M. Tavayef, *et al*., Phys. Lett. B, **781**, 195 (2018). https://doi.org/10.1016/j.physletb.2018.04.001
[25] H. Moradpour, *et al*., Phys. Lett. B, **783**, 82 (2018). https://doi.org/10.1016/j.physletb.2018.06.040
[26] S. Abe, Phys. Rev. E, **63**, 061105 (2001). https://doi.org/10.1103/PhysRevE.63.061105
[27] A. Majhi, Phys. Lett. B, **775**, 32 (2017). https://doi.org/10.1016/j.physletb.2017.10.043

[28] T.S. Biro, and V.G. Czinner, Phys. Lett. B, **726**, 861 (2013). https://doi.org/10.1016/j.physletb.2013.09.032

[29] V.G. Czinner, and H. Iguchi, Phys. Lett. B, **752**, 306 (2016). https://doi.org/10.1016/j.physletb.2015.11.061

[30] N. Komatsu, Eur. Phys. J. C, **77**, 229 (2017). https://doi.org/10.1140/epjc/s10052-017-4800-2

[31] H. Moradpour, *et al.*, Phys. Rev. D, **96**, 123504 (2017). https://doi.org/10.1103/PhysRevD.96.123504

[32] A. Renyi, "On Measures of Entropy and Information," in: *Proceedings of the Fourth Berkeley Symposium on Mathematical Statistics and Probability*, (Berkley, 1961). pp. 547-561.

[33] R.G. Cai, *et al.*, Class. Quantum Grav. **26**, 155018 (2009). https://doi.org/10.1088/0264-9381/26/15/155018

[34] S. Chunlen, and P. Rangdee, (2020). https://arxiv.org/abs/2008.13730

[35] U.Y.D. Prasanthi, and Y. Aditya, Res.Phys. **17**, 103101 (2020). https://doi.org/10.1016/j.rinp.2020.103101

[36] U.K. Sharma, and V.C. Dubey, New Astronomy, **80**, 101419 (2020). https://doi.org/10.1016/j.newast.2020.101419

[37] V.C. Dubey, *et al.*, Astrophys. Space Sci. **365**, 129 (2020). https://doi.org/10.1007/s10509-020-03846-x

[38] V.C. Dubey, and U.K. Sharma, New Astronomy, **86**, 101586 (2021). https://doi.org/10.1016/j.newast.2021.101586

[39] A.A. Mamon, *et al.*, Eur. Phys.J. C, **80**, 974 (2020). https://doi.org/10.1140/epjc/s10052-020-08546-y

[40] A.A. Mamon, *et al.*, Eur. Phys. J. **136**, 134 (2021). https://doi.org/10.1140/epjp/s13360-021-01130-7

[41] U.K. Sharma, *et al.*, Int. J. Mod.Phys. D, **30**, 2150021 (2021). https://doi.org/10.1142/S0218271821500218

[42] U.K. Sharma, and V.C. Dubey, Int. J.Mod.Phys. D, **19**, 2250010 (2022). https://doi.org/10.1142/S0219887822500104

[43] M.V. Santhi, and T. Chinnappalanaidu, New Astronomy, **92**, 101725 (2022). https://doi.org/10.1016/j.newast.2021.101725

[44] M.V. Santhi, *et al.*, Ind. J. Phys. **98**, 3393 (2024). https://doi.org/10.1007/s12648-023-03051-w

[45] C.W. Misner, *et al.*, *Gravitation*, (W.H. Freeman and Company, New York, 1973).

[46] R.D. Inverno, *Introducing Einstein's Relativity*, (Oxford University Press, Oxford, 1998).

[47] A.R. Liddle, *An Introduction to Modern Cosmology*, (Wiley and Sons, Chichester, 2015).

[48] A.R. Liddle, and D.H. Lyth, *Cosmological Inflation and Large-Scale Structure*, (Cambridge University Press, Cambridge, 2000). https://doi.org/10.1017/CBO9781139175180

[49] C.W. Misner, Astrophys. J. **151** 431 (1968). https://doi.org/10.1086/149448

[50] R.K. Kantowski, and R.K. Sachs, J. Math. Phys. **7**, 443 (1966). https://doi.org/10.1063/1.1704952

[51] E. Ghorani, and Y. Heydarzade, Eur.Phys. J. C, **81**, 557 (2021). https://doi.org/10.1140/epjc/s10052-021-09355-7

[52] M.V. Santhi, and T.C. Naidu, Indian J. Phys. **96**, 953 (2022). https://doi.org/10.1007/s12648-020-01983-1

[53] G. Oliveira-Neto, *et al.*, Brazil. J. Phys. **52**, 130 (2022). https://doi.org/10.1007/s13538-022-01137-0

[54] U.Y.D. Prasanthi, and Y. Aditya, Phys. Dark Uni. **31**, 100782 (2021). https://doi.org/10.1016/j.dark.2021.100782

[55] A.A. Shaikh, and D. Chakraborty, J. Geom. Phys. **160**, 103970 (2021). https://doi.org/10.1016/j.geomphys.2020.103970

[56] M. Altunbas, J. Geom. **113**, 40 (2022). https://doi.org/10.1007/s00022-022-00655-1

[57] K.J. Nordtvedt, Astrophys J. **161**, 1059 (1970). https://doi.org/10.1086/150607

[58] J. Schwinger, *Particles, Sources and Fields*, (Addison-Wesley, Reading, 1970). https://archive.org/details/particlessources0001schw

[59] P. Jordan, in: *Schwerkraft und Weltall*, (Friedrich Vieweg and Sohn, Braunschweig, 1955). pp.207-213.

[60] C.H. Brans, and R.H. Dicke, Phys. Rev. **124**, 925 (1961). https://doi.org/10.1103/PhysRev.124.925

[61] V.U.M. Rao, and D. Neelima, Iran. J.Phys. Res. **14**(3), 35 (2014). https://ijpr.iut.ac.ir/article_1085_a67b4dc9c472767d094a4c561fd7475f.pdf?lang=en

[62] V. U. M. Rao., D. Neelima, *Int. Sch. Res. Notices.* **2013**, 174741 (2013). http://dx.doi.org/10.1155/2013/174741

[63] V.U.M. Rao, and D. Neelima, *Int. Sch. Res. Notices.* **2013**, 759274 (2013). https://doi.org/10.1155/2013/759274

[64] V.U.M. Rao, and D. Neelima, *J. Theor. Appl. Phys.* **7**, 50 (2013). https://doi.org/10.1186/2251-7235-7-50

[65] A.R. Solomon, and M. Trodden, *J. Cosmo. Astro. Phys.* **02**, 031 (2018). https://doi.org/10.1088/1475-7516/2018/02/031

[66] Q. Huang, *et al.*, Anna. Phys. **399**, 124 (2018). https://doi.org/10.1016/j.aop.2018.09.014

[67] J. Bloomfield, J. Cosmol. Astropart. Phys. **12**, 044 (2013). https://doi.org/10.1088/1475-7516/2013/12/044

[68] M. López, *et al.*, J. Cosmo. Astro. Phys. **2021**, (2021). https://doi.org/10.1088/1475-7516/2021/10/021

[69] R. Caldwell, and E.V. Linder, Phys. Rev. Lett. **95**, 141301 (2005). https://doi.org/10.1103/PhysRevLett.95.141301

[70] M.V. Sahni, *et al.*, Phys. Rev. D, **78**, 103502 (2008). https://doi.org/10.1103/PhysRevD.78.103502

[71] M.V. Sahni, *et al.*, J. Exp.The.l Phys. Let. **77**(5), 201 (2003). https://doi.org/10.1134/1.1574831

[72] U. Alam, *et al.*, Mon. Not. R. Astron.Soc. **344(4)**, 1057 (2003). https://doi.org/10.1046/j.1365-8711.2003.06871.x

ЕВОЛЮЦIЯ ВСЕСВIТУ КАНТОВСЬКОГО-САКСА З ГОЛОГРАФIЧНОЮ ТЕМНОЮ ЕНЕРГIЄЮ РЕНI

Т. Чиннаппаланайду[a], **С. Шривані Мадху**[a], **М. Віджая Санті**[b], **N. Шрі Лакшмі Судха Рані**[b,c], **А. Крішна Рао**[d]
[a] *Кафедра математики, Інститут інформаційних технологій Віньяна (автономний), Вішакхапатнам 530049, Індія*
[b] *Кафедра прикладної математики, Університет Андхра, Вішакхапатнам 530003, Індія*
[c] *Кафедра гуманітарних наук та природничих наук, Інженерний коледж Тігала Крішна Редді, Хайдерабад 500097, Індія.*
[d] *Кафедра математики, Державний коледж, Чодаварам, Андхрапрадеш, 531036, Індія*

Розглядаючи узагальнену скалярно-тензорну теорію як гравітаційну теорію, ми дослідили динамічну еволюцію однорідного та анізотропного простору Кантовського-Сакса за наявності голографічної темної енергії Реньї. Щоб отримати розв'язок для цієї моделі, ми вивели рівняння поля, а також проаналізували різні фізичні та геометричні параметри моделі, такі як уповільнення, ривок, EoS, площина EoS, пара statefinder, густина, квадрат швидкості звуку та Om-діагностика. Ці параметри показують, що модель є дуже стабільною, проектуючи квінтесенційну природу, а також отримана модель відображає модель ΛCDM. Наші спостереження та висновки з побудованої моделі добре узгоджуються з нещодавніми дослідженнями.

Ключові слова: *метрика Кантовського-Сакса; анізотропні моделі; загальна скалярно-тензорна теорія; голографічна темна енергія Реньї; темна енергія*